Meta-QTL Analysis for Stripe Rust Resistance in Wheat

Irfat Jan
  Ch. Charan Singh University

Gautam Saripalli
  Ch. Charan Singh University

Kuldeep Kumar
  Ch. Charan Singh University

Anuj Kumar
  Ch. Charan Singh University

Rakhi Singh
  Ch. Charan Singh University

Ritu Batra
  Ch. Charan Singh University

Pradeep Kumar Sharma
  Ch. Charan Singh University

Harindra Singh Balyan
  Ch. Charan Singh University

Pushpendra Kumar Gupta (✉ pkgupta36@gmail.com)
  Ch. Charan Singh University   https://orcid.org/0000-0001-7638-6171

Research Article

Abstract

Stripe rust caused by Puccinia striiformis f. sp. tritici Eriks. & E. Henn (Pst) is one of the most prevalent wheat diseases causing upto 70% yield losses worldwide. The present study was conducted in wheat for the first time to identify important meta-QTL (MQTL) regions for their use in developing stripe rust resistant wheat cultivars and to understand the genetic architecture of stripe rust resistance in wheat. For this purpose, a dense consensus map consisting of 76,753 markers was constructed and 353 QTLs from earlier studies were projected on this consensus map. As many as 61 MQTLs were identified using 184 (out of 353) original QTLs. Ten important genomic regions including six breeders' MQTLs (PVE >20%) and four MQTL hotspots were selected to be used by wheat breeders. As many as 409 important candidate genes (CGs) were also identified, which either encoded known R proteins (265) or showed differential expression (144) due to stripe rust infection. These included genes encoding the following proteins: NBS-LRR, WRKY domains, ankyrin repeat domains, sugar transporters, etc. Overall, the present study provided robust MQTLs and underlying CGs which may be potential targets for molecular breeding for development of stripe rust resistant wheat cultivars or may be the target for future molecular studies to understand the mechanism of stripe rust resistance.

Key Message

Important meta-QTL regions and underlying candidate genes were first time identified for stripe rust resistance in wheat for development of resistant cultivars.

Introduction

Due to its wide adaptability, wheat is grown on > 200 mha globally and it provides 20% of the daily protein for the growing world population (Shiferaw et al. 2013; Tesfaye et al. 2021). In production, globally wheat is the second most important crop after maize (FAO-2021). Rust diseases (leaf rust, stem rust and stripe rust) which occur world-wide are among the major biotic stresses severely affecting wheat yield. Among the three rusts, stripe rust (also known as yellow rust or Yr) caused by *Puccinia striiformis* f. sp. tritici Eriks. & E. Henn (Pst) is the most devastating and widely prevalent disease in major wheat growing countries around the world. There are at least 140 stripe rust pathotypes known globally, of these, more than 28 pathotypes occurring in India alone (Line and Qayoum 1992; Chen et al. 2010; Bhardwaj et al. 2014; Tomar et al. 2014; Pradhan et al. 2020).

Stripe rust causes significant yield losses in almost every part of the world, where cool and humid conditions persist during crop season. The yield losses can be up to 70% under severe epidemic conditions, adversely affecting grain-filling duration, thus leading to poor grain yield as well as grain quality (Vikram et al. 2021). Under severe conditions, the yield losses may go up to 100% when the infection occurs at the seedling stage and environment conditions conducive to the pathogen persist until maturity (Afzal et al. 2007; Pradhan et al. 2020). In India, it is a major disease in the North West Plain Zones (NWPZ) especially in the sub-mountainous parts of Punjab, Haryana, and Western Uttar Pradesh,

which are the major wheat growing areas. In fact, a major outbreak of this disease was witnessed in NWPZ during 2006 and in the Northern Hills Zone (NHZ) during 2012-13, leading to severe yield losses (Prashar et al. 2007; Saharan et al. 2013; Pradhan et al. 2020).

As many as 83 Yr genes have already been identified globally, which are distributed on all the 21 wheat chromosomes (McIntosh et al. 2014). Out of these 83 Yr genes, more than 15 genes have been derived from alien wheat species (Park 2016). As many as 9 genes (*Yr5/YrSP, Yr7, Yr10, Yr15, Yr36, Yr18, YrU1* and *Yr46*) have also been cloned and were shown to encode a variety of proteins including those with the nucleotide binding site leucine rich repeats (NBS-LRR) domain, kinase like domains, ankyrin repeats, WRKY domain and lipid binding domain; Yr genes encoding putative ABC transporter and hexose transporter are also known (Fu et al. 2009; Krattinger et al. 2009; Liu et al. 2014; Moore et al. 2015; Klymiuk et al. 2018; Marchal et al. 2018; Zhang et al. 2019; Wang et al. 2020). In the host, a number of differentially expressed genes have also been identified through genome-wide transcriptome analysis during wheat-Pst interaction (Coram et al. 2008; Garnica 2013; Zhang et al. 2014; Hao et al. 2016; Zhang et al. 2019; Pradhan et al. 2020 and Yan et al. 2021) and a network pathway operating during the interaction was also speculated in one of these studies (Zhang et al. 2014).

Stripe rust resistance has also been treated as a quantitative trait (QT) and > 300 QTLs for this trait have been reported using interval mapping (Wang et al. 2017a). Several LD-based genome wide association studies (GWAS) for stripe rust resistance have also been conducted during the last two decades, leading to identification of a number of marker trait associations (MTAs). The activity involving quantitative genetic studies for this trait increased so extensively in recent years that five of these GWA studies were reported in 2021 alone (Zhang et al. 2021; Abou-Zeid et al. 2021; Gyawali et al. 2021; Vikram et al. 2021 and Wu et al. 2021).

However, no attempts have been made so far to conduct MQTL analysis and to validate the robustness of QTLs for stripe rust resistance, identified across different environments and using different mapping populations differing in their genetic make-up. This is despite the fact that MQTL analysis in wheat has been conducted for a number of other traits including those for tolerance to abiotic stresses such as drought and heat (Acuñ
a-Galindo et al. 2015; Kumar et al. 2020) and resistance to biotic stresses like (i) leaf rust (Soriano and Royo 2015), (ii) tan spot (Liu et al. 2020), (iii) stem rust (Yu et al. 2014), (iv) Fusarium head blight (Loffler et al. 2009) and (v) powdery mildew (Marone et al. 2013). The present study involving MQTL analysis is the first of its kind which was planned to identify MQTLs for stripe rust resistance, using the QTL information already available. The CGs for MQTLs were also identified. The MQTLs, MQTL hotspots and the CGs identified during the present study should serve as an important resource for future molecular breeding programs for stripe rust resistance in bread wheat. The results of this study should also allow identification of the consensus and robust QTLs and for refining the QTL positions on a consensus map (Goffinet and Gerber 2000).

Materials And Methods

Bibliographic search and input file preparation

For conducting MQTL analysis for stripe rust resistance, bibliographic search was done to collect literature on QTL mapping studies published during past 20 years (2000 to 2020) (Table S1). From the literature, detailed information on types of mapping populations and their parents, population size, pathotypes used for phenotyping, methods of QTL mapping, position of QTL and markers flanking the QTL, logarithm of odds (LOD) value, and R^2 values of the QTLs was collected. Only QTLs with complete information required for meta-analysis were retained for final analysis. The two types of input data text files including the genetic map file and QTL information file were prepared from each study following the instructions provided in the BioMercator v3/v4 manual (Sosnoswki and Joets 2012).

Construction of consensus genetic map

A consensus genetic map involving SSR, DArT and SNP markers was constructed using LPmerge software (Endelman and Plomion 2014). For this purpose, five individual genetic linkage maps each from different studies were used as reference maps (Somers et al. 2004; Marone et al. 2012; Maccaferri et al. 2014; Wang et al. 2014 and Bokore et al. 2020). Markers flanking individual QTL regions identified in individual QTL studies used for MQTL analysis were also included for construction of a consensus genetic map.

Projection of QTLs on consensus map

The original QTLs were projected onto the above developed consensus map using the QTL projection (QTL Proj) tool available in BioMercator v4.2; QTLs which could not be projected onto the consensus map were excluded. For the projection of QTLs on the consensus map, a scaling rule between the marker interval of the original QTL and the corresponding interval on the consensus chromosome was used (Veyrieras et al. 2007). The new confidence interval (CI) for MQTLs on the consensus linkage group was computed using Gaussian distribution (Veyrieras et al. 2007).

Meta-analysis of QTLs and identification of MQTL hotspots

MQTL analysis was conducted using BioMercator v4.2 (Arcade et al. 2004; Sosnowski et al. 2012). Following two different approaches were used based on the number of QTLs on each individual chromosome for conducting MQTL analysis: (i) If the number of QTLs on an individual chromosome was ≤10, the approach suggested by Goffinet and Gerber (2000) was used; and (ii) if the number of QTLs on an individual chromosome was >10, the approach suggested by Veyrieras et al. (2007) was used. For identification of the MQTLs, QTL model having the lowest Akaike information criterion (AIC) value was considered (AIC value estimates the relative amount of data lost by different statistical models). Quality of the model depended on the assumption that lesser is the information loss, higher will be the quality of that model (Akaike 1998). The MQTLs located in the same physical interval and genetic/confidence interval <15 cM were considered as MQTL hotspots.

Identification of known Yr genes co-located with MQTLs

The known Yr genes that are co-located with the MQTLs in the present study were also identified. For this purpose, the sequences of the markers linked to the Yr genes were blasted against the wheat reference genome version 49 (*Triticum_aestivum* IWGSC_Ensembl_Release 49) available in the Ensembl Plants database and the physical coordinates of the respective markers were extracted. These physical intervals of the markers linked to Yr genes were compared with the physical coordinates of the MQTL regions; an individual Yr gene falling within a specific MQTL region was treated as the MQTL region co-located with the corresponding Yr gene.

Identification of CGs underlying the MQTL regions

The CGs underlying the MQTL regions were identified in the 1Mb interval on either side of the peak position of the MQTL (total 2Mb interval). For this purpose, the options available in biomart tool of Ensembl Plants were utilized. The following steps were used to identify CGs: (i) the physical coordinates of the MQTLs were extracted by Blasting the sequences of the closest markers (retrieved from GrainGenes, CerealDB or JBrowse) flanking the MQTL regions against the wheat reference genome sequence (*Triticum_aestivum* IWGSC_Ensembl_Release 49) available in Ensembl Plants database. (ii) The physical interval (in Mb) for an individual MQTL was calculated based on the genetic confidence interval (in cM) of the MQTL regions. For this purpose, the genetic interval (in cM) was divided by the physical interval (in Mb, calculated from the coordinate information of the MQTL and the distance in units of Mb per cM was calculated. (iii) Based on this information, the actual physical position of the MQTL was calculated and the 1Mb region on either side of the MQTL (total 2Mb interval) was extended for identification of the putative CGs associated with the respective MQTL region. (iv) The putative function of the identified CGs was annotated on the basis of the domain in their protein sequences, which were identified utilizing InterPro database.

Gene ontology (GO) and *in silico* expression analysis of CGs

GO analysis was conducted using Biomart tool available in Ensemble Plants. *In silico* expression of CGs was also conducted using the tool expVIP available online (wheat-expression.com; Ramirez-Gonzalez et al. 2018) to select the important genes based on their expression values. Expression data on three different experiments involving two different studies related to stripe rust resistance that were available in expVIP database were selected for *in silico* expression analysis. Following is the brief summary of these two expression studies. In the first study conducted by Zhang et al. (2014), transcriptome divergence and overlap in response to stripe rust and powdery mildew was studied using the seven-day old seedlings of the variety N9134 that was inoculated using Pst race CYR31. The inoculated leaves were harvested at 0, 1, 2, and 3 dpi (Zhang et al. 2014). In the second study of Dobon et al. (2016), two different varieties, namely Vuka (susceptible) and Avocet-*Yr5* (resistant) were inoculated with stripe rust using Pst isolate 87/66 at three leaf stage. Leaf samples were collected at 0, 1, 2, 3, 5, 7, 9, and 11 days post-inoculation (dpi) for the susceptible variety Vuka and 0, 1, 2, 3, and 5 dpi for the resistant Avocet-*Yr5* line. In both the studies, three biological replicates were taken for each time point.

The data on expression was available as log2 transformed tpm (transcripts per million) values. Only those genes showing FC≥2 or FC≤-2 (on comparison of tpm values under stress vs. control) were considered as differentially expressed. The results of such differentially expressed genes were depicted in the form of heatmaps generated using online tool Morpheus (https://software.broadinstitute.org/morpheus/).

Results

QTLs and their distribution on wheat chromosomes

Based on the bibliographic search, a total of 68 studies (66 studies involving common wheat and two studies involving durum wheat) were found to contain all the required QTL related information and were used for the MQTL analysis (Table 1; for details see Table S1). Salient features of these studies include the following: (i) The mapping populations consisting of RILs, DH or F_3 ranged in size from 78 to 1020 plants/lines (Table1; Table S1). (ii) A total of 353 QTLs were identified from these 68 studies and the information on the flanking marker, phenotypic variation explained (PVE) % of each QTL along with their confidence intervals (CI) are presented in Table S1. (iii) The 353 QTLs were distributed on the all the 21 wheat chromosomes, with the total number of QTLs per chromosome ranging from 3 on chromosome 5D to 52 on chromosome 2B (Figure 1a). (iv) Of the QTLs, 100 (28.3%) QTLs were identified on A sub-genome, 206 (58.4%) on B sub-genome and 47 (13.3%) on D sub-genome (Figure 1a). The number of QTLs per trait ranged from 2 for leaf area infected (LAI) to 243 for disease severity (DS) (Figure 1b). (iv) LOD scores for these QTLs ranged from 2 to 62 with 47% of QTLs showing a LOD score of 2-7 (Figure 1c). (v) The proportion of phenotypic variance explained (PVE) by individual QTLs ranged from 1% to 88% (average of 6%) and followed the expected L-shaped distribution, with most (67%) of the QTLs showing a PVE <20 % (Figure 1d).

Consensus map and projection of QTLs on consensus map

The consensus map had 76,753 markers, including 3526 DArT, 65459 SNP, 3975 SSR, and 3793 AFLP, STS, and TRAP etc. The total length of the consensus map was 5774 cM; the size of the 21 individual linkage groups ranged from 98 cM to 462 cM (Figure 2). The marker densities ranged from 5 markers per cM in case of 6D to 28 markers per cM for 1A (Figure 2). The average marker densities of the seven linkage groups was the lowest for D sub- genome (11.85 markers per cM) followed by B sub-genome (14.28 markers per cM) and A sub-genome (15.42 markers per cM) (Figure 2).

Out of the total 353 QTLs collected from 68 studies, only 214 QTLs could be projected on to the consensus map; only these were used for MQTL analysis.

MQTLs, MQTL hotspots and their distribution on wheat chromosomes

Out of the 214 QTLs projected on the consensus map, 30 QTLs were found to be singletons and were therefore removed from further analysis. The remaining 184 QTLs with 8 QTLs overlapping two adjacent

MQTLs were grouped into 61 MQTLs following the lowest AIC values. These MQTLs were located on 18 out of the 21 chromosomes (except 5D, 6D and 7D) with 1 to 8 MQTLs per chromosome (Figure 3). Further, all original QTLs clustered in each of the 60 out of the 61 MQTL regions (except MQTL57) were identified using different types of mapping populations reported in different studies. In case of MQTL57 which was represented by 2 initial QTLs, both these QTLs were reported from the same population in a single study (Table 2). For 59 out of the 61 MQTLs, the information of stripe rust pathotypes that were utilized during the original studies was also available. The number of individual QTLs per MQTL ranged from 2 to 10 (Table 2). Mean R^2 (PVE %) of the MQTLs ranged from 1.9% to 48.1% and their CI ranged from 0.02 cM (MQTL51) to 11.47 cM (MQTL40). Out of the 61 MQTLs, maximum (36) MQTLs were found on the B sub-genome followed by 19 MQTLs on A sub-genome and 6 MQTLs on D sub-genome. The genetic position, genetic interval and other related information for each MQTL are listed in Table S2.

Four MQTL hotspot regions were identified on chromosome 1B, 2B and 6B. Each of the four hotspot regions consisted of 2 MQTLs as follows: (i) MQTL4-1B and MQTL5-1B containing 9 initial QTLs controlling 6 different traits (ii) MQTL14-2B and MQTL15-2B containing 5 initial QTLs controlling single trait and 7 known Yr genes (iii) MQTL17-2B and MQTL18-2B containing 15 initial QTLs controlling 5 different traits and 9 known Yr genes and (iv) MQTL53-6B and MQTL54-6B containing 6 initial QTLs controlling 3 different traits (Figure 3; Table 2).

Co-located Yr genes with the MQTLs

Twenty-two (22) known major Yr genes were found to be co-located (on the basis of physical position of MQTLs as well as the physical position of Yr genes) within the genomic regions of the following 10 MQTLs; MQTL3, 10, 15, 17, 18, 19, 20, 21, 24 and 29; 9 Yr genes were co-located with MQTL3 alone (Figure 3). Further, since the physical intervals of the MQTL15, MQTL17 and MQTL21 overlapped with each other, the same six Yr genes were co-located with these three MQTLs. In case of MQTL17, one more gene was co-located in addition to these six genes.

Identification of CGs, GO terms and *in-silico* expression analysis

A total of 1581 genes were available in the genomic regions defined by 60 out of the 61 MQTLs. Of the above 1581 genes, total 409 (265+144) important CGs were identified based on two different criteria which included (i) 265 important R genes which follow six of the 9 different mechanisms listed by Kourellis and van der Hoorn (2018) (Figure 4a and Table S3) and (ii) 144 significant differential expression based on *in silico* expression analysis (Table S4). These 265 genes belonged to 48 out of the 61 MQTLs. Twenty four (24) of the above 144 differentially expressed genes mentioned in category 1 were also commonly identified in the 265 genes belonging to second category.

GO analysis of the above 409 (144+265) CGs revealed a number of GO terms out of which some of the important and most abundant GO terms include those involved in biological processes like phosphorylation, protein ubiquitination, proteolysis, transmembrane transport, oxidation-reduction processes, etc. Similarly, important GO terms in molecular functions category included those involved in

catalytic activity, ATP binding, protein binding, heme binding, iron ion binding, metal ion binding, transmembrane transporter activity, oxidoreductase activity, etc.

The above 144 differentially expressed CGs identified through *in silico* expression analysis (FC≥2 or ≤-2) belonged to 44 out of 60 MQTLs and the number of differentially expressed genes per MQTL ranged from 1 to 8 (Table 3 and Table S4). Further, these differentially expressed CGs encoded proteins for different categories like R-domain containing proteins, transcription factors (Zn finger binding proteins, SANT/Myb domains, NAC domain, BTF3), transporters (mitochondrial carrier domains, sugar-phosphate transporter domain, sodium/carbon exchanger domain, SLC26A/SulP transporter), different protein kinases, genes involved in calcium signaling, a number of peptidases, genes involved in oxidative stress (cytochrome P450) and domains like S1/P1 nuclease, Six-bladed beta-propeller/Strictosidine synthase, Alpha-mannosyltransferase and Peptidase T2 (Table S4). A representative heat map of 29 important differentially expressed CGs which included 14 CGs encoding R domain containing proteins, 9 CGs known to be involved in disease resistance signaling pathways and 6 CGs having very high expression (FC≥ 5 or ≤-5) shown in Figure 4b.

Discussion

The QTL interval mapping studies for stripe rust in wheat started in mid-1990s (Line et al. 1996). Since then, more than 70 reports have been published, leading to identification of >350 QTLs, so that stripe rust resistance is now treated both as a quantitative trait involving quantitative resistance loci (QRLs) and a qualitative trait controlled by a number of Yr genes, the latter following a gene-for-gene relationship with Avr genes in the pathogen. The relationship of QRLs in the host and the corresponding QTLs for virulence in the pathogen has not been worked out so far, although quantitative nature of virulence in pathogen has been worked out in some cases including wheat pathogens like *Zymoseptoria tritici* where several large and small effect QTLs were identified for virulence (Stewart et al. 2018)

The 61 MQTLs identified during the present study were derived from 184 QTLs, which indicated roughly three-times reduction in redundancy for the genomic regions controlling stripe rust resistance in wheat genome. Earlier, while conducting meta-QTL analysis in wheat for fusarium head blight, roughly five-fold reduction in redundancy was reported (Venske et al. 2019). The absence of MQTLs on the 3 of the 7 D sub-genome chromosomes (5D, 6D, 7D; Figure 2) agrees with earlier reports on QTL analysis (Gutierrez-Gonzalez et al. 2019; Rimbert et al. 2018; Gardener et al. 2016; Iehisa et al. 2016; Poland et al. 2012). A similar situation was earlier reported for MQTL analysis for leaf rust resistance (Soriano and Royo 2015) and MQTLs for fusarium head blight (Venske et al. 2019).

Sixty-one (61) MQTLs (including four MQTLs derived from the QTLs belonging to durum wheat) is a fairly large number indicating a high degree of redundancy of QTLs which agrees with a large number of Yr genes for stripe rust resistance reported in wheat genome. Such a redundancy of genes/MQTLs is a requirement for providing resistance against large number of ever-evolving races of stripe rust, distributed in different wheat growing regions of the world (Pradhan et al. 2020). Earlier, for resistance against

fusarium head blight also, 65 MQTLs were identified. However, the number of MQTLs identified in this study far exceeds the number of MQTLs identified for leaf rust resistance (35) (Soriano and Royo 2015). Perhaps this is due to relatively fewer QTL studies (19) available for meta-analysis in case of leaf rust resistance.

Most of the MQTLs identified in the present study controlled more than one parameters/traits (Table 2; Table S2). This probably indicated either a tight linkage of genes for different traits, or occurrence of pleotropic genes or a bias due to the use of related traits measuring the same resistance component by different means as also reported earlier in case of MQTL analysis for leaf rust resistance in wheat (Soriano and Royo 2015). In the present study, five MQTLs (MQTL3-1B, MQTL10-2A, MQTL19-2B, MQTL20-2B and MQTL24-2D) also showed co-localization of 1 to 9 different known Yr genes including four cloned Yr genes. These genomic regions may be involved in controlling both, qualitative and quantitative resistance and thus may be more important. Earlier, a number of Yr genes (out of the 82 reported Yr genes) have been deployed in commercial wheat cultivars; however only few are still effective. For instance, some of the Yr genes which are still effective in India include *Yr5, Yr10, Yr15, Yrsp, Yr47, Yr57* and *Yr63* (Prasad 2020; Sharma et al. 2020). Four of these Yr genes (*Yr5, Yr10, Yr15, Yrsp*) that were found to be co-located with MQTLs (Figure 3) identified during the present study and four other Yr genes (*Yr53, Yr61, Yr65,Yr69)* are known to be effective worldwide (Zhang et al. 2019; Zhou et al. 2014). The MQTLs showing co-localization with Yr genes may be important targets for introgression into susceptible wheat lines for improvement of stripe rust resistance. While breeding for stripe rust resistance, generally Yr genes are deployed and there is only one report where two QTL (*QYr.nafu-2BL* and *QYr.nafu-3BS*) have been utilized for developing stripe rust resistance in wheat cultivars (Hu et al. 2020).

Some of the MQTLs also overlap Yr genes that have already been cloned. For instance, MQTL20-2B was co-localized with two cloned Yr genes (*Yr5/Yrsp* and *Yr7*) whereas MQTL1-1A was co-localized with cloned gene *Yr10*. Co-localization of *Yr5/Yrsp* and *Yr7* in the same MQTL region is perhaps due to the allelic nature of both the genes which were earlier shown to be closely linked (Zhang et al. 2009). All the above three cloned genes encode proteins for NBS-LRR (Liu et al. 2014; Marchal et al. 2018).

Efforts were also made during the present study to identify MQTLs and MQTL hot spots that may prove useful for breeding; we describe these MQTLs as breeders' MQTL. For selecting these breeders' MQTLs, we utilized a number of criteria including the following two criteria suggested in an earlier study (Loffler et al. 2009): (i) the low CI and high average PVE of the MQTLs and (ii) the number of QTLs carried by individual MQTL. Additional criteria were also used in the present study for prioritizing and selecting breeders' MQTLs and MQTL hotspots. For instance, the relationship between MQTLs and the pathotypes occurring in specific wheat growing regions may be an important criterion. While doing this we also have to keep in mind that virulence can also be quantitative in nature as mentioned earlier. MQTLs showing resistance against more than one pathotypes may also be important for achieving broad spectrum resistance. Such important MQTLs showing resistance against multiple pathogen races were also identified in a recent study on MQTL analysis reported for tan spot resistance in wheat (Liu et al. 2020).

MQTLs identified in the present study consisted of original QTLs which showed resistance at either APR, HTAP (high temperature adult plant resistance), SR (seedling resistance) or all stage resistance (ASR). Also, almost all the MQTLs (except MQTL36-4A) showed resistance against more than one pathotypes indicating that these MQTLs exhibit race non-specific resistance and may be containing a number of novel genes which may be involved in providing resistance against broad spectrum of pathotypes. Keeping in view the different criteria listed above, a number of breeders' MQTLs were identified, which are listed in Table 4.

Some of the Yr genes have been shown to overlap the QRLs/MQTLs and also the CGs that were identified during the present study. The 409 CGs identified during the present study have been shown to encode a variety of proteins; at least some of them are known to be involved in disease resistance (Table 3). The differential expression of CGs observed during the present study agrees with earlier reports (Wang et al 2021; Dobon et al. 2016; Zhang et al. 2014). These genes are largely involved in important processes like protein phosphorylation, photosynthesis, protein ubiquitination, transmembrane transport, oxidation-reduction processes, etc. which are relevant to disease resistance. In an earlier study also, a reduction in photosynthesis was shown to enhance stripe rust resistance due to the interaction of *Yr36*, encoding for *wheat kinase START1* (*WKS1*) with Psbo, a member of photosystem II (Wang et al. 2019) without having any adverse effect on yield. Similarly, in another study, a number of genes encoding PR (pathogenesis-related) proteins, involved in a number of defense responses were shown to get induced in response to stripe rust infection in a number of wheat lines carrying different genes for ASR (*YrTr1, Yr76, YrSP, YrExp2*) and HTAP (*Yr5, Yr59, Yr62* and *Yr7b*) (Farrakh et al. 2016). A number of downstream genes, apparently similar to the CGs identified in the present study and involved in processes mentioned above were also identified in a transcriptome study conducted using a pair of introgression lines, which differed for *Yr5* (Dobon et al. 2016).

CGs identified during the present study also deserve to be discussed. In wheat, CGs underlying the MQTLs were also identified for several traits including drought tolerance (Kumar et al. 2020), tan spot resistance (Liu et al. 2020) and fusarium head blight resistance (Venske et al. 2019). However, the strategy used by us was novel and not used in any of these earlier reports. For instance, in most of the earlier reports, the complete physical interval of the MQTL regions was considered for identification of CGs. However, in the present study, we calculated the exact physical position of the MQTL based on the MQTL peak position available from the BioMercator software. The 1 Mb interval on either sides of the MQTL peak was considered for identification of genes, which were used for identification of CGs responsible for stripe rust resistance.

Important differentially expressed CGs identified in the present study are presented in Figure 4. Fifty-nine (59) CGs out of the total 409 CGs were available in breeder's MQTL indicating that these CGs are more important. Out of the 59 CGs, 32 CGs also showed differential expression and encoded important R genes, S/TPK, SLC transporter, Mitogen-activated protein (MAP) kinase, UDP-glucosyltransferases, S1/P1 nuclease, etc. The role of some of the important CGs (shown in Figure 4) during disease resistance can be summarised as follows: (i) Earlier, *STPK-V*, a member of *Pm1* gene was reported to confer powdery

mildew resistance in wheat (Cao et al. 2011). (ii) NBS-LRR domain containing genes are the protein products of the cloned Yr genes like *Yr10, Yr5*, etc. as mentioned earlier (Liu et al. 2014; Marchal et al. 2018). (iii) *TaMAPK4*, a type of MAPK gene is reported to act as a positive regulator of stripe rust resistance in wheat (Wang et al. 2018). (iv) The above transporters may also possibly encode Yr genes similar to *Yr46* which was shown to encode for hexose transporter (Moore et al 2015). (v) UDP-glucosyltransferases were earlier reported to show differential expression due to stripe rust infection in wheat genotypes indicating their role in *Yr39* mediated stripe rust resistance (Coram et al. 2008). Some other important CGs like those encoding for WRKY domains, Ankyrin repeat and F-box domain containing genes were also identified in different MQTLs, although the expression data was not available for these genes. WRKY and Ankyrin repeat domain containing genes were recently found to encode for proteins of cloned *YrU* gene (Wang et al. 2020). Similarly, F-box domain containing gene was identified as a CGs underlying the *YrR39* locus in wheat and it was shown to upregulate due to stripe rust infection (Yin et al. 2018).

In summary, the present study allowed us to identify 6 MQTLs and 4 MQTL hotspots to be used by breeders particularly for high yielding wheat cultivars which are susceptible for stripe rust (Table 4). Four of these 10 genomic regions also showed co-localization with known Yr genes. Some of the important CGs which were identified during the present study may be further validated/edited using approaches like gene editing, overexpression, gene knockout strategies or CG based association mapping (CGAM). Reports are available where some of these strategies have been used for validation of genes for their role in stripe rust resistance. For instance, overexpression of *TaWRKY62* provided high temperature seedling plant resistance to stripe rust by activating other genes encoding for PR proteins, salicylic and jasmonic acid responsive genes and ROS associated genes (Wang et al. 2017b). Similarly, in another study overexpression of *TaLHY* (a type pf MYB TF) in leaf blade and sheath reduced the negative impacts of stripe rust on wheat plant (Zhang et al. 2015). This knowledge may prove to be useful for validating similar CGs identified in this study.

Gene editing or mutation is still unexplored in case of stripe rust resistance except a single study where the function of *Yr15* gene (encoding *wheat tandem kinase 1* or *WKS1*) in stripe rust resistance was validated using mutation analysis (Klymiuk et al. 2020). EMS mutations were created in this gene in resistant wheat lines to develop susceptible lines. The resulting susceptible lines showed point mutations in the three amino acids,i.e. Gly54, Ala149 and Ala460 leading to disruption in gene function, thereby validating the role of *WSK1* in resistance. Therefore, a similar strategy may be certainly explored for at least three cloned genes (*Yr5/Yrsp, Yr7* and *Yr10*) which are co-located in two important MQTL regions mentioned in Table 4 as well the important CGs shown in Figures 4a and 4b. Similarly, techniques involving CRISPR/Cas9 or base editing may also be employed for the above cloned Yr genes as well as the CGs after the identification of causal SNPs involved in providing stripe rust resistance through CGAM approach. Similar report involving CRISPR/Cas9 for fusarium head blight are available where successful editing (using CRISPR-Cas9) of three genes, *TaABCC6, TaNFXL1*, and *TansLTP9* showed enhanced resistance (Cui et al. 2017).

Declarations

Author contributions PKG, HSB and PKS conceived and planned this study. IJ, KK, AK, RS and RB collected the literature and tabulated the data for meta-QTL analysis. IJ conducted the meta-QTL analysis using Biomercator software. IJ and GS interpreted the results and wrote the manuscript. PKG, HSB, and PKS edited and finalised the manuscript with the help of IJ and GS.

Compliance with ethical standards

Conflicts of interest

The authors declare no conflicts of interest.

Availability of Data and Material Additional data relevant to this paper is available as supplementary information.

Code availability Not applicable

References

1. Abou-Zeid MA, Mourad AM (2021) Genomic regions associated with stripe rust resistance against the Egyptian race revealed by genome-wide association study. BMC Plant Biol 21:1–4

2. Acuña-Galindo MA, Mason RE, Subramanian NK, Hays DB (2015) Meta-analysis of wheat QTL regions associated with adaptation to drought and heat stress. Crop Sci 55:477–492

3. Afzal SN, Haque MI, Ahmedani MS, Bashir S, Rattu AR (2007) Assessment of yield losses caused by *Puccinia striiformis* triggering stripe rust in the most common wheat varieties. Pak J Bot 39:2127–2134

4. Akaike HA (1998) Bayesian analysis of the minimum AIC procedure. InSelected papers of Hirotugu Akaike. Springer, New York, pp 275–280

5. Arcade A, Labourdette A, Falque M, Mangin B, Chardon F, Charcosset A, Joets J (2004) BioMercator: integrating genetic maps and QTL towards discovery of candidate genes. Bioinformatics 20:2324–2326

6. Bhardwaj SC, Prashar M, Prasad P (2014) Ug99-future challenges. In: Future challenges in crop protection against fungal pathogens. Springer, New York, pp 231–247

7. Bokore FE, Knox RE, Cuthbert RD, Pozniak CJ, McCallum BD, N'Diaye A, DePauw RM, Campbell HL, Munro C, Singh A, Hiebert CW (2020) Mapping quantitative trait loci associated with leaf rust

resistance in five spring wheat populations using single nucleotide polymorphism markers. Plos One 15:e0230855

8. Buels R, Yao E, Diesh CM, Hayes RD, Munoz-Torres M, Helt G, Goodstein DM, Elsik CG, Lewis SE, Stein L, Holmes IH (2016) JBrowse: a dynamic web platform for genome visualization and analysis. Genome Biol 17:1–2

9. Cao A, Xing L, Wang X, Yang X, Wang W, Sun Y, Qian C, Ni J, Chen Y, Liu D, Wang X (2011) Serine/threonine kinase gene *Stpk-V*, a key member of powdery mildew resistance gene *Pm21*, confers powdery mildew resistance in wheat. Proc Natl Acad Sci 108:7727–7732

10. Chen X, Penman L, Wan A, Cheng P (2010) Virulence races of *Puccinia striiformis* f. sp. *tritici* in 2006 and 2007 and development of wheat stripe rust and distributions, dynamics, and evolutionary relationships of races from 2000 to 2007 in the United States. Can J Plant Pathol 32:315–333

11. Coram TE, Settles ML, Chen X (2008) Transcriptome analysis of high-temperature adult-plant resistance conditioned by *Yr39* during the wheat–*Puccinia striiformis* f. sp. *tritici* interaction. Mol Plant Pathol 9:479–493

12. Cui X. Targeted gene editing using CRISPR/Cas9 in a wheat protoplast system (Doctoral dissertation, Université d'Ottawa/University of Ottawa)

13. Dobon A, Bunting DC, Cabrera-Quio LE, Uauy C, Saunders DG (2016) The host-pathogen interaction between wheat and yellow rust induces temporally coordinated waves of gene expression. BMC Genom 17:1–4

14. Endelman JB, Plomion C (2014) LPmerge: an R package for merging genetic maps by linear programming. Bioinformatics 30:1623–1624

15. Farrakh S, Wang M, Chen X (2018) Pathogenesis-related protein genes involved in race-specific all-stage resistance and non-race specific high-temperature adult-plant resistance to *Puccinia striiformis* f. sp. *tritici* in wheat. J Integr Agric 17:2478–2491

16. Fu D, Uauy C, Distelfeld A, Blechl A, Epstein L, Chen X, Sela H, Fahima T, Dubcovsky J (2009) A kinase-START gene confers temperature-dependent resistance to wheat stripe rust. Science 323:1357–1360

17. Gardner KA, Wittern LM, Mackay IJ (2016) A highly recombined, high-density, eight-founder wheat MAGIC map reveals extensive segregation distortion and genomic locations of introgression segments. Plant Biotech J 14:1406–1417

18. Garnica DP, Upadhyaya NM, Dodds PN, Rathjen JP (2013) Strategies for wheat stripe rust pathogenicity identified by transcriptome sequencing. Plos One 8:e67150

19. Goffinet B, Gerber S (2000) Quantitative trait loci: a meta-analysis. Genetics 155:463–473

20. Gutierrez-Gonzalez JJ, Mascher M, Poland J, Muehlbauer GJ (2019) Dense genotyping-by-sequencing linkage maps of two Synthetic W7984× Opata reference populations provide insights into wheat structural diversity. Sci Rep 9:1–5

21. Gyawali S, Mamidi S, Chao S, Bhardwaj SC, Shekhawat PS, Selvakumar R, Gangwar OP, Verma RP (2021) Genome-wide association studies revealed novel stripe rust resistance QTL in barley at

seedling and adult-plant stages. Euphytica 217:1–8

22. Hao Y, Wang T, Wang K, Wang X, Fu Y, Huang L et al (2016) Transcriptome Analysis Provides Insights into the mechanisms underlying wheat plant resistance to stripe rust at the adult plant stage. Plos One 11:e0150717

23. Hu T, Zhong X, Yang Q, Zhou X, Li X, Yang S, Hou L, Yao Q, Guo Q, Kang Z (2020) Introgression of two quantitative trait loci for stripe rust resistance into three Chinese wheat cultivars. Agronomy 10:483

24. Iehisa JC et al (2014) A high-density genetic map with array-based markers facilitates structural and quantitative trait locus analyses of the common wheat genome. DNA Res 21:555–567

25. Klymiuk V, Yaniv E, Huang L, Raats D, Fatiukha A, Chen S, Feng L, Frenkel Z, Krugman T, Lidzbarsky G, Chang W (2018) Cloning of the wheat *Yr15* resistance gene sheds light on the plant tandem kinase-pseudokinase family. Nat Commun 9:1–2

26. Kourelis J, Van Der Hoorn RA (2017) Defended to the nines: 25 years of resistance gene cloning identifies nine mechanisms for R protein function. Plant Cell 30:285–299

27. Krattinger SG, Lagudah ES, Spielmeyer W, Singh RP, Huerta-Espino J, McFadden H, Bossolini E, Selter LL, Keller B (2009) A putative ABC transporter confers durable resistance to multiple fungal pathogens in wheat. Science 323:1360–1363

28. Kumar A, Saripalli G, Jan I, Kumar K, Sharma PK, Balyan HS, Gupta PK (2020) Meta-QTL analysis and identification of candidate genes for drought tolerance in bread wheat (*Triticum aestivum* L.). Physiol Mol Biol Plants 26:1713–1725

29. Line RF, Chen XM, Gale MD, Leung H (1996) Development of molecular markers associated with quantitative trait loci in wheat for durable resistance to *Puccinia striiformis*. Proc 9th European and Mediterranean Cereals Rust and Mildew Conf, Lunteren, The Netherlands, p 234

30. Line RF, Qayoum A (1992) Virulence, aggressiveness, evolution, and distribution of races of *Puccinia striiformis* (the cause of stripe rust of wheat) in North America, 1968-87. Technical bulletin-United States Department of Agriculture1788:44

31. Liu W, Frick M, Huel R, Nykiforuk CL, Wang X, Gaudet DA, Eudes F, Conner RL, Kuzyk A, Chen Q, Kang Z (2014) The stripe rust resistance gene *Yr10* encodes an evolutionary-conserved and unique CC–NBS–LRR sequence in wheat. Mol Plant 7:1740–1755

32. Liu Y, Salsman E, Wang R, Galagedara N, Zhang Q, Fiedler JD, Liu Z, Xu S, Faris JD, Li X (2020) Meta-QTL analysis of tan spot resistance in wheat. Theor Appl Genet 133:2363–2375

33. Löffler M, Schön CC, Miedaner T (2009) Revealing the genetic architecture of FHB resistance in hexaploid wheat (*Triticum aestivum* L.) by QTL meta-analysis. Mol Breed 23:473–488

34. Maccaferri M, Cane MA, Sanguineti MC, Salvi S, Colalongo MC, Massi A, Clarke F, Knox R, Pozniak CJ, Clarke JM, Fahima T (2014) A consensus framework map of durum wheat (*Triticum durum* Desf.) suitable for linkage disequilibrium analysis and genome-wide association mapping. BMC Genom 15:1–21

35. Marchal C, Zhang J, Zhang P, Fenwick P, Steuernagel B, Adamski NM, Boyd L, McIntosh R, Wulff BB, Berry S, Lagudah E (2018) BED-domain-containing immune receptors confer diverse resistance

spectra to yellow rust. Nat Plant 4:662–668

36. Marone D, Laido G, Gadaleta A, Colasuonno P, Ficco DB, Giancaspro A, Giove S, Panio G, Russo MA, De Vita P, Cattivelli L (2012) A high-density consensus map of A and B wheat genomes. Theor Appl Genet 125:1619–1638

37. Marone D, Russo MA, Laidò G, De Vita P, Papa R, Blanco A, Gadaleta A, Rubiales D, Mastrangelo AM (2013) Genetic basis of qualitative and quantitative resistance to powdery mildew in wheat: from consensus regions to candidate genes. BMC Genom 14:1–7

38. McIntosh RA, Dubcovsky J, Rogers JW, Morris CF, Appels R, Xia XC (2014) Catalogue of gene symbols for wheat: 2013-14 Supplement. Annual wheat newsletter 58

39. Moore JW, Herrera-Foessel S, Lan C, Schnippenkoetter W, Ayliffe M, Huerta-Espino J, Lillemo M, Viccars L, Milne R, Periyannan S, Kong X (2015) A recently evolved hexose transporter variant confers resistance to multiple pathogens in wheat. Nat Genet 47:1494–1498

40. Park RF (2016) Wheat: Biotrophic pathogen resistance. In: Encyclopedia of Food Grains, 2nd edn Academic Press, pp 264–272

41. Poland JA, Brown PJ, Sorrells ME, Jannink JL (2012) Development of high-density genetic maps for barley and wheat using a novel two-enzyme genotyping-by-sequencing approach. Plos One 7:e32253

42. Pradhan AK, Kumar S, Singh AK, Budhlakoti N, Mishra DC, Chauhan D, Mittal S, Grover M, Kumar S, Gangwar OP, Kumar S, Gupta A, Bhardwaj SC, Rai A, Singh K (2020) Identification of QTLs/defense genes effective at seedling stage against prevailing races of wheat stripe rust in India. Front Genet 11

43. Prasad P, Gangwar OP, Kumar S, Bhardwaj SC (2020) Mehtaensis: Six monthly newsletter named after Prof. KC Mehta 40:6

44. Prashar M, Bhardwaj SC, Jain SK, Dutta D (2007) Pathotypic evolution in *Puccinia striiformis* in India during 1995–2004. Aust J Agric Res 58:602–604

45. Ramírez-González RH, Borrill P, Lang D, Harrington SA, Brinton J, Venturini L, Davey M, Jacobs J, Van Ex F, Pasha A, Khedikar Y (2018) The transcriptional landscape of polyploid wheat. Science 361:6403

46. Rimbert H et al (2018) High throughput SNP discovery and genotyping in hexaploid wheat. Plos One 13:e0186329

47. Saharan MS, Selvakumar R, Sharma I (2013) Wheat Crop Health Newsletter 18:1–8

48. Sharma A, Srivastava P, Mavi GS, Kaur S, Kaur J, Bala R, Sohu VS, Chhuneja P, Bains NS (2021) Resurrection of wheat cultivar 'PBW343'using marker assisted gene pyramiding for rust resistance. Front Plant Sci 12:42

49. Shiferaw B, Smale M, Braun HJ, Duveiller E, Reynolds M, Muricho G (2013) Crops that feed the world 10. Past successes and future challenges to the role played by wheat in global food security. Food Secur 5:291–317

50. Somers DJ, Isaac P, Edwards K (2004) A high-density microsatellite consensus map for bread wheat (*Triticum aestivum* L.). Theor Appl Genet 109:1105−1114

51. Soriano JM, Royo C (2015) Dissecting the genetic architecture of leaf rust resistance in wheat by QTL meta-analysis. Phytopathol 105:1585−1593

52. Sosnowski O, Charcosset A, Joets J (2012) BioMercator V3: an upgrade of genetic map compilation and quantitative trait loci meta-analysis algorithms. Bioinformatics 28:2082−2083

53. Stewart EL, Croll D, Lendenmann MH, Sanchez-Vallet A, Hartmann FE, Palma-Guerrero J, Ma X, McDonald BA (2018) Quantitative trait locus mapping reveals complex genetic architecture of quantitative virulence in the wheat pathogen *Zymoseptoria tritici*. Mol Plant Pathol 19:201−216

54. Tesfaye K (2021) Climate change in the hottest wheat regions. Nature Food 2:8−9

55. Tomar SM, Singh SK, Sivasamy M (2014) Wheat rusts in India: resistance breeding and gene deployment-a review. Indian J Genet Plant Breed 74:129−156

56. Venske E, Dos Santos RS, Farias DD, Rother V, da Maia LC, Pegoraro C, Costa de Oliveira A (2019) Meta-analysis of the QTLome of Fusarium head blight resistance in bread wheat: refining the current puzzle. Front Plant Sci 10:727

57. Veyrieras JB, Goffinet B, Charcosset A (2007) MetaQTL: a package of new computational methods for the meta-analysis of QTL mapping experiments. BMC Bioinformatics 8:1−6

58. Victoria C, Blake MR, Woodhouse GR, Lazo, Sarah G, Odell, Charlene P, Wight, Nicholas A, Tinker Y, Wang YQ, Gu CL, Birkett J-L, Jannink, Dave E, Matthews, David L, Hane SL, Michel E, Yao, Taner Z Sen (2019) GrainGenes: centralized small grain resources and digital platform for geneticists and breeders, Database, Volume, 2019, baz065

59. Vikram P, Sehgal D, Sharma A, Bhavani S, Gupta P, Randhawa M et al (2021) Genome-wide association analysis of Mexican bread wheat landraces for resistance to yellow and stem rust. Plos One 16:e0246015

60. Wang B, Song N, Zhang Q, Wang N, Kang Z (2018) *TaMAPK4* acts as a positive regulator in defense of wheat stripe-rust infection. Front Plant Sci 9:152

61. Wang H, Zou S, Li Y, Lin F, Tang D (2020) An ankyrin-repeat and WRKY-domain-containing immune receptor confers stripe rust resistance in wheat. Nat Commun 11:1−1

62. Wang J, Tao F, Tian W, Guo Z, Chen X, Xu X, Shang H, Hu X (2017b) The wheat WRKY transcription factors *TaWRKY49* and *TaWRKY62* confer differential high-temperature seedling-plant resistance to *Puccinia striiformis* f. sp. *tritici*. Plos One 12:e0181963

63. Wang M, Chen X (2017a) Stripe rust resistance. In: Stripe Rust. Springer, Dordrecht, pp 353−558

64. Wang S, Wong D, Forrest K, Allen A, Chao S, Huang BE, Maccaferri M, Salvi S, Milner SG, Cattivelli L, Mastrangelo AM (2014) Characterization of polyploid wheat genomic diversity using a high-density 90 000 single nucleotide polymorphism array. Plant Biotechnol J 12:787−796

65. Wang S, Li QP, Wang J, Yan Y, Zhang GL, Zhang H, Wu J, Chen F, Wang X, Kang Z, Dubcovsky J (2019) *YR36/WKS1*-mediated phosphorylation of PsbO, an extrinsic member of photosystem II,

inhibits photosynthesis and confers stripe rust resistance in wheat. Mol Plant 12:1639–1650

66. Wang Y, Huang L, Luo W, Jin Y, Gong F, He J, Liu D, Zheng Y, Wu B (2021) Transcriptome analysis provides insights into the mechanisms underlying wheat cultivar Shumai126 responding to stripe rust. Gene 768:145290

67. Wilkinson PA, Allen AM, Tyrrell S, Wingen LU, Bian X, Winfield MO, Burridge A, Shaw DS, Zaucha J, Griffiths S, Davey RP (2020) CerealsDB—new tools for the analysis of the wheat genome: update 2020. Database 2020

68. Wu J, Yu R, Wang H, Zhou CE, Huang S, Jiao H, Yu S, Nie X, Wang Q, Liu S, Weining S (2021) A large-scale genomic association analysis identifies the candidate causal genes conferring stripe rust resistance under multiple field environments. Plant Biotechnol J 19:177–191

69. Yan X, Zheng H, Zhang P, Weldu GT, Li Z, Liu D (2021) QTL mapping of adult plant resistance to stripe rust in the Fundulea 900× Thatcher RIL population. Czech J Genet Plant Breed 57:1–8

70. Yin JL, Fang ZW, Sun C, Zhang P, Zhang X, Lu C, Wang SP, Ma DF, Zhu YX (2018) Rapid identification of a stripe rust resistant gene in a space-induced wheat mutant using specific locus amplified fragment (SLAF) sequencing. Sci Rep 8:1–9

71. Yu LX, Barbier H, Rouse MN, Singh S, Singh RP, Bhavani S, Huerta-Espino J, Sorrells ME (2014) A consensus map for Ug99 stem rust resistance loci in wheat. Theor Appl Genet 127:1561–1568

72. Zhang C, Huang L, Zhang H, Hao Q, Lyu B, Wang M, Epstein L, Liu M, Kou C, Qi J, Chen F (2019) An ancestral NB-LRR with duplicated 3' UTRs confers stripe rust resistance in wheat and barley. Nat Commun 10:1–2

73. Zhang H, Yang Y, Wang C, Liu M, Li H, Fu Y, Wang Y, Nie Y, Liu X, Ji W (2014) Large-scale transcriptome comparison reveals distinct gene activations in wheat responding to stripe rust and powdery mildew. BMC Genomics 15:1–4

74. Zhang P, McIntosh RA, Hoxha S, Dong C (2009) Wheat stripe rust resistance genes *Yr5* and *Yr7* are allelic. Theor Appl Genet 20:25–29

75. Zhang P, Yan X, Gebrewahid TW, Zhou Y, Yang E, Xia X, He Z, Li Z, Liu D (2021) Genome-wide association mapping of leaf rust and stripe rust resistance in wheat accessions using the 90K SNP array. Theor Appl Genet 25:1–9

76. Zhang Z, Chen J, Su Y, Liu H, Chen Y, Luo P, Du X, Wang D, Zhang H (2015) *TaLHY*, a 1R-MYB transcription factor, plays an important role in disease resistance against stripe rust fungus and ear heading in wheat. Plos One 10:e0127723

77. Zhou XL, Han DJ, Chen XM, Gou HL, Guo SJ, Rong L, Wang QL, Huang LL, Kang ZS (2014) Characterization and molecular mapping of stripe rust resistance gene *Yr61* in winter wheat cultivar Pindong 34. Theor Appl Genet 127:2349–2358

Tables

Table 1. A summary of QTL studies used for MQTL analysis (details are provided in Table S1)

No. of lines (range of population size; no. of studies)	Parameters	Pathotypes used	Methods of QTL analysis
I. Recombinant inbred lines (RILs)			
59 (92-288; 47)	AUDPC, IT, DS, SR, NDVI, LP, RT	CYR23, CYR29, CYR30, CYR31, CYR32, CYR33, CYR34, CYR34(V26), PSTv-3, PSTv-4, PSTv-8, PSTv-11, PSTv-14, PSTv-17, PST-25, PST-29, PST-35, PSTv-37, PSTv-40, PSTv-41, PSTv-43, PSTv-45, PSTv-49, PSTv-48, PSTv-51, PSTv-53, PST-54, PST-V26, PST-100, PST-102, PST-114, PST-115, PST-116, PST-127, AB50-2, AB7-2, G2214, Mex96.11, Mex08.13, Mex14.191, MX-94.11, V26/CH42, V26/Gui22-9, Su11-7, 6E22A+, 6E16A-, 6E22A-, V2, 46S102, 46S103, 46S119, 134E16A+, 134E16A+Yr17+, 134E16A+J+T+, 237E141, 46S119, 237E141, 237E141V17	ICIM, CIM, SMA, LOCO-LMM, MIM
II. Doubled haploid (DH)			
19 (78-1020; 14)	IT, DS, SR, IR,AUDPC,RT,NDVI, LAI	PSTv-37, C-PST-2, C-PST-30, 6E22A+, 106E139, CYR29, CYR31, CYR32, CYR33, Shui4, Shui5, Hy8, Shui4, Shui6, Hy6, Hy7, 6E22A+, 71/93, 08/97, 70/99, 6E22A-, Mex96.11, 110E143A+	ICIM, CIM
III. F$_3$ lines			
7 (136-326; 7)	IT, AUDPC, DS, SN	CYR29, CYR31, CYR32, CYR33, PST-Su5, PST-CH42, PST-Hy8, PST-V26WYR76/10, WYR92/1, WYR68-1, PST-1, PST-21, Shui4, Shui5, Hy8, Shui6, Hy6, Hy7	ICIM, SIM, CIM

RIL: recombinant inbred line, DH: doubled haploid, AUDPC: area under disease progress curve, IT: infection type, DS: disease severity, SR: stripe rust response, NDVI: normalized difference vegetation index, LP: latency period, RT: reaction type, IR: infection response, LAI: leaf area infected, SN: number of stripes per 10 cm^2 leaf area, ICIM: inclusive composite interval mapping, CIM: composite interval mapping, SMA: single marker analysis, LOCO-LMM: leave one chromosome out-linear mixed model, MIM: multiple interval mapping, SIM: simple interval mapping

Table 2. A summary of the results of MQTL analysis for stripe rust resistance in wheat. (For details, see Table S2)

MQTL-Chromosome	Interval (cM/Mb)	Peak pos. (cM)/ Mean R^2	QTL studies; QTLs represented by MQTL (no. of pathotypes)	Traits associated with the MQTL
MQTL1-1A	8.90-10.10/6.34-584.36	9.48/9.6	4; 4 (3)	DS,IT
MQTL2-1A	62-71.80/483.52-510.46	66.84/8.2	2; 2 (3)	DS
MQTL3-1B	45.31-48.99/660.56-687.79	47.15/27.6	2; 2 (7)	DS,IT
MQTL4-1B	58.91-60.37/394.03-394.33	59.64/15.15	3; 3 (5)	IT,SR,IR,DS,NDVI
MQTL5-1B	64.41-64.71/398.15-571.19	64.56/23.94	6; 6 (12)	IT,DS,AUDPC,NDVI
MQTL6-1B	94.73-95.23/189.34-678.74	94.98/27.35	3; 3 (7)	DS,IT
MQTL7-1B	148.29-148.93/667.21-667.60	148.61/9.8	3; 3 (9)	DS
MQTL8-1B	186.28-189/439.01-670.78	187.64/34.2	2; 2 (4)	DS,IT
MQTL9-1D	0.08-2.93/7.84-423.26	1.5/5.8	2; 2 (3)	DS
MQTL10-2A	5.72-13.22/2.50-36.85	9.47/45	5; 5 (16)	DS,IT
MQTL11-2A	54.38-56.40/18.29-27.44	55.39/14.15	5; 5 (8)	AUDPC,DS
MQTL12-2A	91.70-92.20/695.18-715.29	91.95/13.3	3; 3 (7)	RT,DS
MQTL13-2A	105.29-106.87/30.87-32.11	106.08/41	2; 2 (5)	DS,AUDPC,IT
MQTL14-2B	14.02-14.92/598.57-680.77	14.47/17.9	2; 2 (3)	DS

MQTL15-2B	20.49-25.64/562.26-673.71	23.06/11.25	3; 3 (4)	DS
MQTL16-2B	50.79-52/0.48-16.83	51.4/45.8	2; 2 (3)	DS,IT
MQTL17-2B	64.70-65.58/42.28-771.17	65.14/14.46	4; 5 (6)	DS
MQTL18-2B	74.16-75.98/764.90-771.17	75.07/29.70	10; 10 (23)	DS,AUDPC,IT,SR,IR
MQTL19-2B	81.76-84.56/554.45-763.84	83.16/21.6	4; 4 (8)	DS,AUDPC,IT
MQTL20-2B	96.40-98.14/687.47-777.14	97.27/40.26	5; 5 (15)	DS,IT,NDVI
MQTL21-2B	180.74-183.64/29.04-672.64	182.19/16.8	2; 2 (3)	DS,IT
MQTL22-2D	71.28-72.56/20.76-26.34	71.92/10.2	2; 2 (3)	AUDPC,DS
MQTL23-2D	96.53-100.20/45.88-57.26	98.37/48.1	2; 2 (2)	LP,IT,DS
MQTL24-2D	124.65-130.6/27.92-132.52	127.62/47.2	3; 3 (6)	AUDPC,DS,IT
MQTL25-3A	1.20-2.76/10.14-11.38	1.98/8.05	3; 3 (2)	LP,IT,DS
MQTL26-3A	58.46-59.39/24.61-32.15	58.92/32.6	3; 3 (5)	DS,IT
MQTL27-3B	0.12-0.70/5.59-6.75	0.41/24.5	2; 2 (6)	DS,IT
MQTL28-3B	3.69-4.67/710.98-773.05	4.18/35.7	3; 3 (2)	DS,IT
MQTL29-3B	21.40-23.70/2.89-7.61	22.55/11.1	3; 3 (4)	SR,IR,DS,RT
MQTL30-3B	32.05-	32.49/15.98	6; 6 (12)	DS,AUDPC,IT

	32.94/15.05-130.42			
MQTL31-3B	42.55-43.64/804.80-811.89	43.09/6.825	3; 3 (9)	IT,DS,NDVI
MQTL32-3B	56.95-59.82/77.49-822.58	58.38/8	4; 4 (10)	DS,AUDPC,IT
MQTL33-3B	90.92-91.48/5.59-739.14	91.2/13.675	4; 5 (9)	DS,AUDPC,IT
MQTL34-3B	152.56-156.68/778.29-814.63	154.62/35	2; 2 (4)	DS
MQTL35-3D	107.50-111.81/47.78-603.46	109.65/11.7	2; 2 (8)	DS,AUDPC,IT
MQTL36-4A	52.94-56.52/591.70-596.31	54.73/11.5	2; 3 (1)	SR,IR,DS
MQTL37-4A	74.39-75.54/615.94-617.99	74.97/7	2; 2 (3)	DS,IT
MQTL38-4A	104.42-105.41/667.35-673.97	104.91/3.5	2; 2 (2)	DS,IT
MQTL39-4A	136.30-140.09/719.18-731.70	138.19/12.85	3; 3 (2)	DS,IT
MQTL40-4B	6.11-17.61/23.46-646.14	11.86/48.5	3; 3 (3)	DS,AUDPC,IT
MQTL41-4B	42.45-43.32/149.04-626.78	42.88/14.275	5; 5 (7)	DS,IT
MQTL42-4D	52.82-63.82/456.36-488.50	58.32/22	2; 2 (10)	DS,AUDPC,IT
MQTL43-5A	65.73-71.43/445.28-458.20	68.58/6.4	2; 2 (3)	AUDPC,DS
MQTL44-5A	88.10-88.97/57.92-595.90	88.53/6.4	2; 2 (10)	SR,AUDPC,DS

MQTL45-5A	126.69-137.69/499.45-698.64	132.19/3.9	2; 2 (NA)	DS,AUDPC,IT
MQTL46-5B	126.99-130.34/8.19-12.33	128.66/10.3	4; 4 (9)	AUDPC,DS
MQTL47-5B	164.88-171.45/44.47-479.39	168.16/13.5	3; 3 (10)	DS,IT
MQTL48-5B	199.02-199.81/695.66-695.79	199.41/6.7	2; 2 (2)	DS
MQTL49-6A	16.18-20.28/14.35-18.71	18.23/4.6	3; 3 (4)	DS,IT
MQTL50-6A	30.25-34.82/17.90-24.07	32.53/10.2	3; 3 (3)	LP,IT,DS,AUDPC
MQTL51-6A	87.35-87.37/448.22-550.64	87.36/1.98	2; 2 (13)	DS,IT
MQTL52-6B	5.80-10.99/398.97-418.14	8.39/4.53	4; 4 (15)	AUDPC,DS
MQTL53-6B	27.23-28.58/680.08-705.29	27.9/21.33	4; 4 (10)	DS,AUDPC,IT
MQTL54-6B	35.59-39.53/690.96-694.13	37.56/4.99	2; 2 (2)	AUDPC
MQTL55-6B	51.48-52.95/708.02-720.98	51.95/25	2; 2 (1)	DS,IT
MQTL56-6B	58.08-63.99/465.68-508.61	61.03/25.85	3; 3 (6)	DS,AUDPC,IT
MQTL57-7A	13.85-15.33/3.78-4.47	14.59/6.3	1; 2 (NA)	DS
MQTL58-7B	57.60-61.61/41.10-421.07	59.6/13.5	2; 2 (2)	DS,IT
MQTL59-7B	97.51-101.40/704.28-709.00	99.45/8.86	5; 5 (8)	AUDPC,DS

| MQTL60-7B | 113.52-116.40/365.38-732.65 | 113.96/5.7 | 2; 2 (2) | DS |
| MQTL61-7B | 136.61-138.42/716.65-717.00 | 137.51/11.3 | 3; 3 (4) | IT,DS |

NA: not available, AUDPC: area under disease progress curve, IT: infection type, DS: disease severity, SR: stripe rust response, NDVI: normalized difference vegetation index, LP: latency period, RT: reaction type, IR: infection response

Table 3. Number of differentially expressed CGs identified through *in silico* expression analysis. (For details of all CGs see Tables S3 and S4).

No. of differentially expressed CGs per MQTL	MQTL with a specific number of expressed CGs, ranging from 1-8 (number of total MQTL)
1	MQTL17, MQTL30, MQTL32, MQTL34, MQTL38, MQTL47, MQTL48, MQTL53, MQTL61 (9)
2	MQTL10, MQTL19, MQTL20, MQTL28, MQTL31, MQTL50, MQTL51 (7)
3	MQTL1, MQTL2, MQTL4, MQTL5, MQTL18, MQTL23, MQTL25, MQTL29, MQTL43, MQTL46, MQTL56, MQTL59, MQTL60 (13)
4	MQTL15, MQTL36, MQTL37 (3)
5	MQTL13, MQTL16, MQTL24, MQTL42, MQTL55, MQTL57 (6)
6	MQTL12, MQTL14, MQTL27 (3)
7	MQTL3, MQTL7 (2)
8	MQTL44 (1)

Table 4. Important MQTLs on the basis of PVE, number of races, traits, initial QTLs and co-located Yr genes

| Important MQTLs (PVE%)	Important features
MQTL10-2A (45), MQTL20-2B(40.26), MQTL24-2D(47.20), MQTL40-4B(48.50)	Pathogen races ≥ 3 and initial QTL ≥ 3 and traits ≥ 2
MQTL18-2B (Yr72), MQTL19-2B (Yr43, Yr44, Yrsp), MQTL20-2B (Yr72, Yr5, Yr7), MQTL24-2D (Yr16)	PVE>20%, pathogen races, initial QTL and trait ≥ 3, co-located Yr genes
MQTL4-1B and MQTL5-1B, MQTL14-2B and MQTL15-2B, MQTL17-2B and MQTL18-2B, MQTL53-6B and MQTL54-6B	MQTL hotspots (MQTLs falling in same physical interval and cM≤15 cM)

Figures
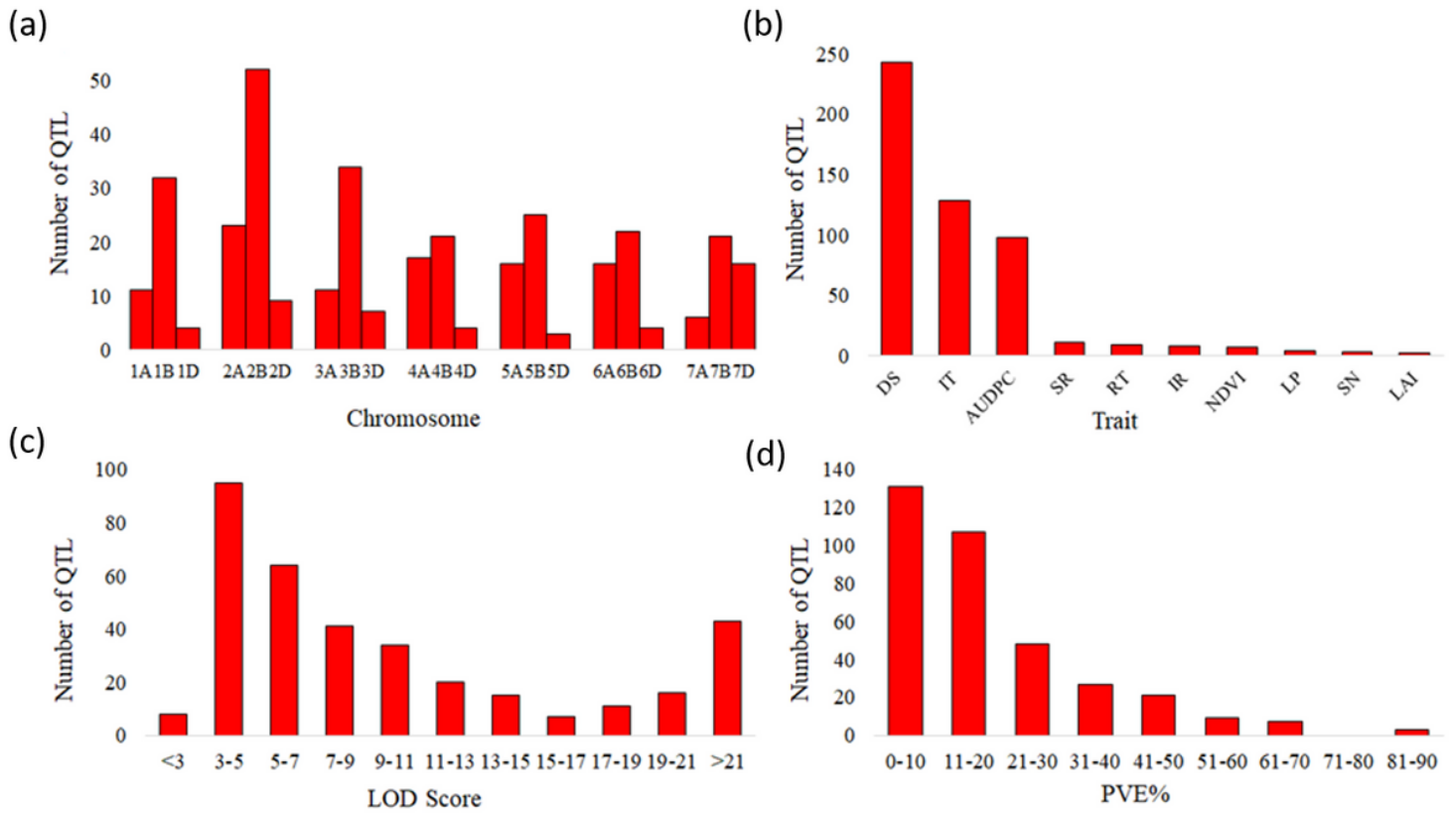
Figure 1

Distribution of QTLs based on (a) chromosome, (b) traits (c) LOD score and (d) phenotypic variance explained (PVE%). DS: disease severity, IT: infection type, AUDPC: area under disease progress curve, SR: stripe rust response, RT: reaction type, IR: infection response, NDVI: normalized difference vegetation index, LP: latency period, SN = stripe number per 10 cm2 leaf area, LAI: leaf area infected.
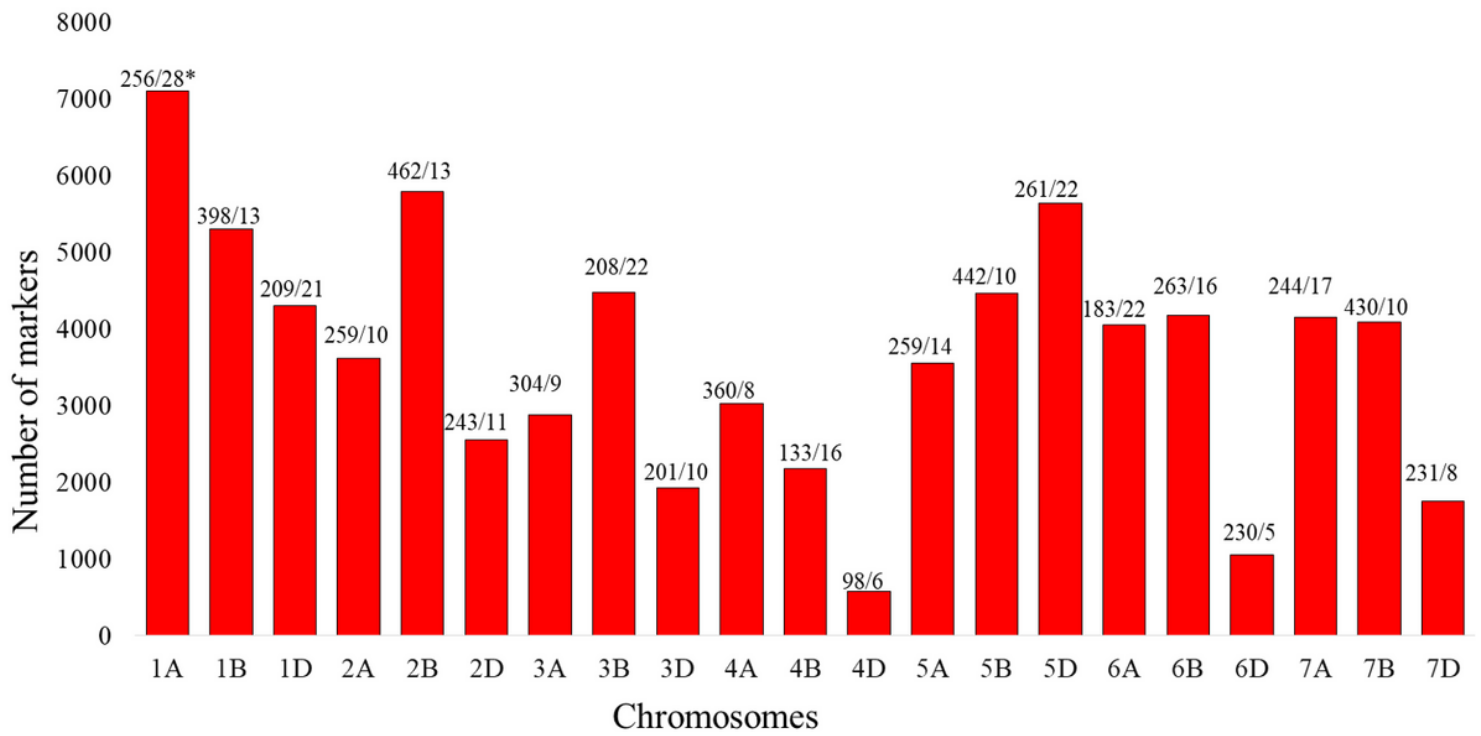
Figure 2

Number of markers on each of the 21 individual wheat chromosomes based on the consensus map used for MQTL analysis. * = chromosome length (in cM)/marker density (markers/cM).
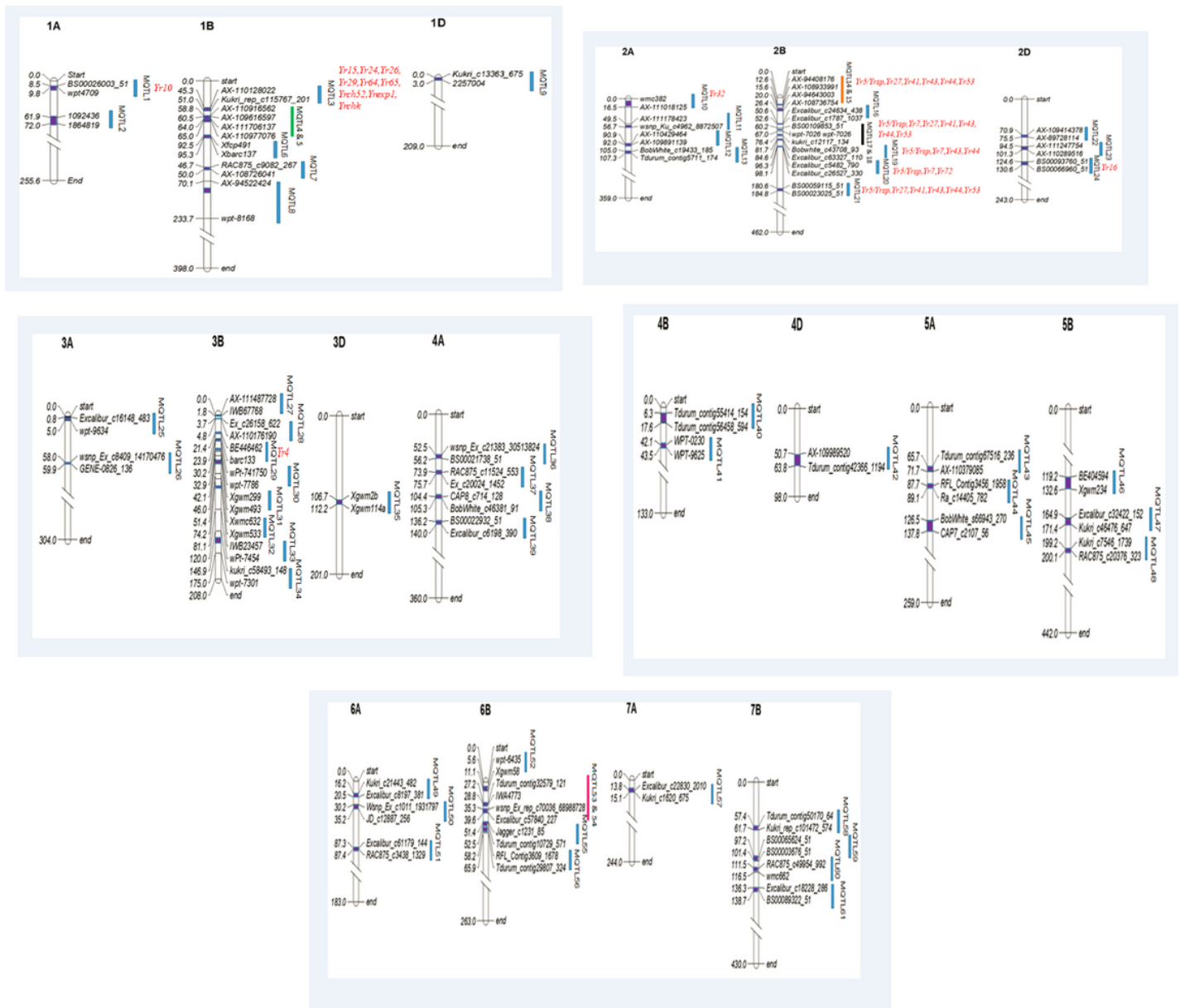
Figure 3

Distribution of 61 MQTLs on 18 of 21 chromosomes (cM) of wheat. The dark blue blocks inside each chromosome indicate MQTL regions and the light blue vertical bars on the right of each chromosomes indicate marker intervals. Marker intervals of QTL hotspots are shown by the shaded bars in green, orange, black and pink colors. Only the flanking markers most closely associated with MQTLs have been shown in the figure. The Yr genes co-located with the MQTLs are indicated in red font.
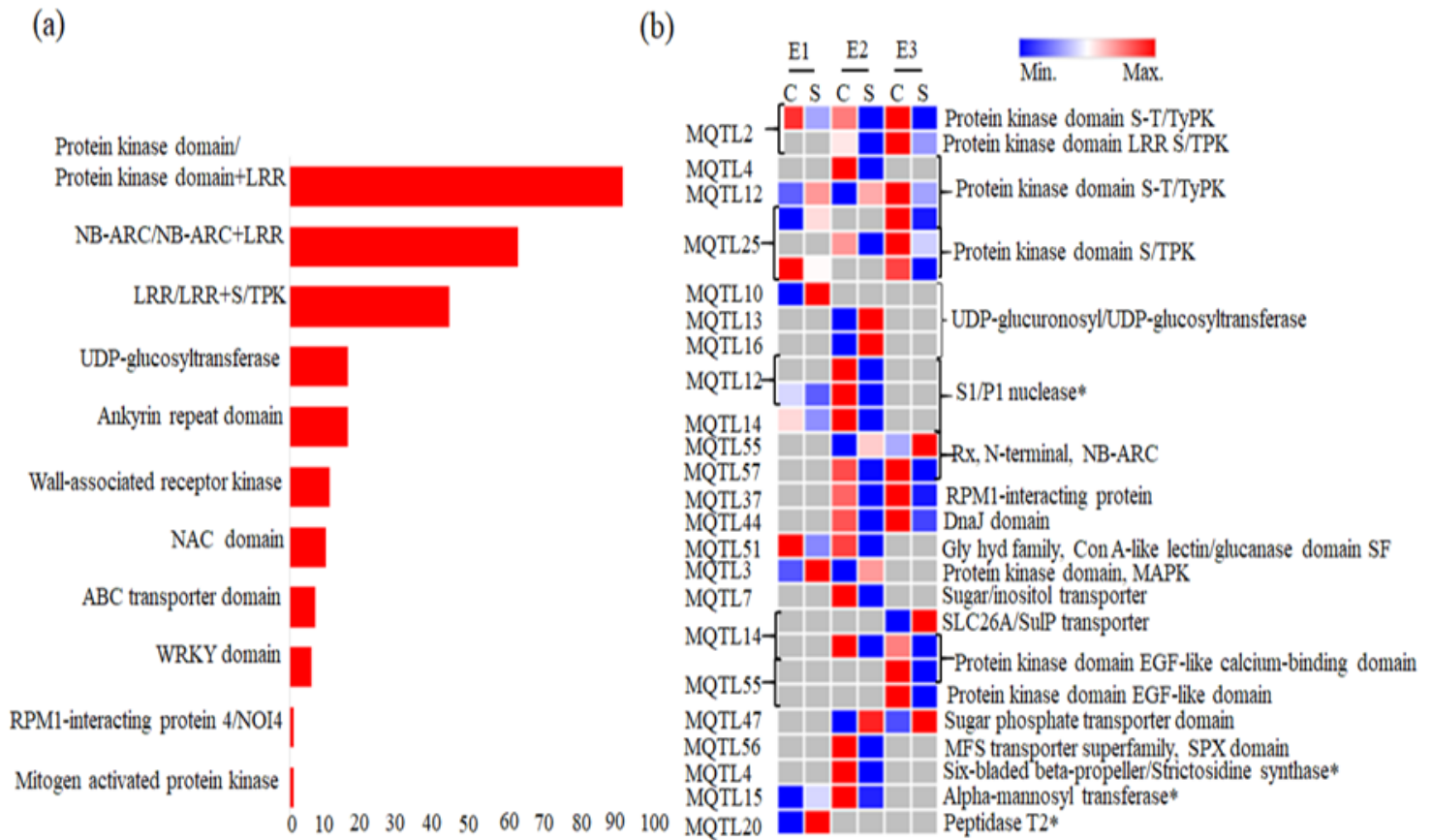
Figure 4

Important candidate genes: (a) histogram showing frequencies of CGs encoding proteins with domains involved in disease resistance; (b) heatmap showing 29 important differentially expressed CGs. C: control, S: stress, E1: experiment 1, E2: experiment 2, E3: experiment 3. S-T/TyPK; serine-threonine/tyrosine protein kinase, S/TPK; serine/threonine protein kinase, LRR; leucine rich repeats. Genes marked with asterix (*) had FC≥5 or ≤-5.

Supplementary Files

This is a list of supplementary files associated with this preprint. Click to download.

- FinalSupplementaryfiles.xlsx